Characterization of Prepreg Initial Morphology

Duffner, C*, Courteau-Godmaire, H, Zobeiry, N and Poursartip, A
Department of Materials Engineering, The University of British Columbia, Vancouver Canada
* Corresponding author (caitlin@composites.ubc.ca)

ABSTRACT

Understanding the initial condition of pre-impregnated composite sheets (i.e., prepreg) assists in predicting manufacturing defects including forming-induced wrinkling and porosity. Several techniques to collectively assess the initial prepreg morphology are presented in this paper. Digital Image Correlation (DIC) strain and change in the height of pre-heated samples show localized non-uniformity that mirror resin and fibre tow placement. Scanning Electron Imaging (SEM) combined with image analysis is used to analyse resin distribution in prepreg cross sections. Infrared Imaging and Optical Microscopy allow visualization of resin distribution patterns on the surface prepreg. Evaluating the common trends seen using this wide variety of tests offers insight into the initial prepreg conditions Although any one technique does not capture the full material morphology, the combined information leads to questions on the impact of the structure on different behaviours.

KEYWORDS: *pre-gelation, non-contact analysis, prepreg morphology*

1 INTRODUCTION

In thermoset composite processing, the material starts as a compliant fabric made of a stiff fibre bed and viscous resin. At this stage, it is easy to manipulate the material, but tampering with its initial state can have a significant impacts later in processing. Studies have reported connections between the initial condition of the material and process induced defects such as wrinkling, porosity, residual stresses (Mohseni et al., 2018; Stewart, 2018; Stewart & Poursartip, 2018). Recent work on the pre-gelation state of material has shown a disconnection between traditional models and the observed physical behaviour (Duffner et al., 2018). The combination of increased research looking at defects induced during early stages of processing and more detailed understanding of the global behaviour of the martial during the pre-gelation state becomes even more relevant as manufacturing techniques such as AFP and forming increase in popularity. With this shift in manufacturing, there is increased interest in developing methods to characterize the raw material.

Recent studies have looked at the surface properties of both out-of-autoclave and autoclave prepreg (Helmus et al., 2017; Lukaszewicz & Potter, 2011) to determine the void content of the material. These studies have used optical techniques to observe the roughness in the material and assess void content. Knowledge of the void content can be used to change processes in order to reduce the likelihood of associated defects.

This study presents several methods that can be used collectively to assess the initial prepreg morphology. Digital Image Correlation (DIC) offers a non-contact measuring technique that captures the local and global behaviour of the in-plane and through-thickness dimensional changes of a prepreg

sample. Optical Microscopy and Infrared (IR) imaging identifies the distribution of resin on the surface while imaging with a Scanning Electron Microscope (SEM) identifies the resin and void distribution through a ply cross-section. By combining information gained from each method, trends in the material structure become apparent and can be used to assume connections between morphology and the response of the material as it is heated.

2 METHODS

2.1 Material

The material used in the study is Hexcel AS4/8552 unidirectional (UD) pre-impregnated (prepreg) material (HexPly AS4 12K/8552;35%;190AW) (HEXCEL, 2016). AS4/8552 is manufactured using a hot melt process. Cure kinetics and viscosity models created from the previous characterization of AS4/8552 was used in RAVEN simulation software (Convergent Manufacturting, 2017; Van Ee & Poursartip, 2009). RAVEN simulations have been implemented in this study to obtain viscosity profiles for testing conditions.

2.2 Digital Image Correlation

Characterizing the pre-gelation stage of the material has proven difficult in the past. Traditional methods for measuring the strain development in composite material, such as a TMA, exert small forces on the samples impacting the pre-gelation response. DIC offers a non-contact approach to measure strain in the prepreg during processing (Duffner et al., 2018). Although previous studies were looking at the average strain development as a sample cured, the same method could be used to look at local variations in the strain at different time steps during heating.

For this study, 1-ply of AS4/8552 prepreg was cut into a 25mm x 25mm x 0.2 mm square sample. A black on white speckle pattern was applied using spray paint. Deformations in the speckle pattern were tracked using image analysis. In addition to the speckle pattern, two sets of three evenly spaced dots were placed 7mm from the top and bottom of the sample. These dots were used as a reference when making cross-section cuts after DIC images have been taken. DIC cameras was set up above the sample angled inward so each camera frame was looking at similar pictures. DIC camera images were captured and analysed using Correlated Solutions VIC-3D software (Correlated Solutions, 2010).

An Anton Paar Peltier heating plate was used to control the temperature of the sample. The Peltier was made of a highly conductive coating. For this experiment, the Peltier is covered with a non-stick Teflon substrate to reduce tool-part interaction (Raffer, 2003).

The temperature cycle used was a fast 10°C/min ramp from 20°C to 60ºC and held at 60°C for 30 minutes before rapidly cooling to 20°C. Images were taken every 30 seconds as the sample was heated. Correlated Solutions software was used to calculate in-plane strains based on deformation of the speckle pattern and the change in the height of the sample. DIC was also used to capture the z-displacement (Δz) of the sample.

2.3 Scanning Electron Microscopy

Once the sample used in the DIC test was cooled, cross-sections of the material were taken using the reference dots placed on the sample. Samples were cut using a thin sharp blade healed at a 30-degree angle. A piece of scotch tape was placed on each sample used to separate any debris left from cutting.

To prepare for imaging, cross-sections were placed in a vacuum chamber overnight to eliminate any off-gassing that could occur in the SEMs pressure chamber. Cross-sections were then mounted on a small aluminium block using carbon tape and sputter coated with gold. A stitched image was taken using an FEI Quanta 650 SEM with an acceleration voltage of 15kV.

2.4 Infrared Imagining

A FLIR IR camera was used to capture the thermal profile of a 40mm x 40mm x.2mm sample of prepreg that had been heated from 20°C to 60 °C at a rate of 10°C/min then held at 60 °C for 5 minutes before being rapidly cooled. IR images were taken immediately after the temperature ramp. The image was taken approximately 100cm from the sample. FLIR software was used to analyze the sample.

2.5 Optical Microscopy

A Keyence VHX-1000 digital microscope was used to observe the surface of the same 40mm x 40mm x.2mm sample of prepreg used for IR imaging after it had been heated to 60 °C for 5 minutes before rapidly cooled.

3 RESULTS AND DISCUSSION

3.1.1 DIC

In our past studies, Digital Image Correlation has been used to capture the global behaviour of prepreg material starting before gelation through cure. These studies have shown that during the pre-gelation region the surface tension of the resin induces self-consolidation of voids thus leading to global shrinkage. In addition to showing the average behaviour of a part over time, the primary method used in the past test, DIC provides a snap-shot of the strain and position on a part at any stage during the processing cycle demonstrating the local behaviour of the material as seen in Figure 1.

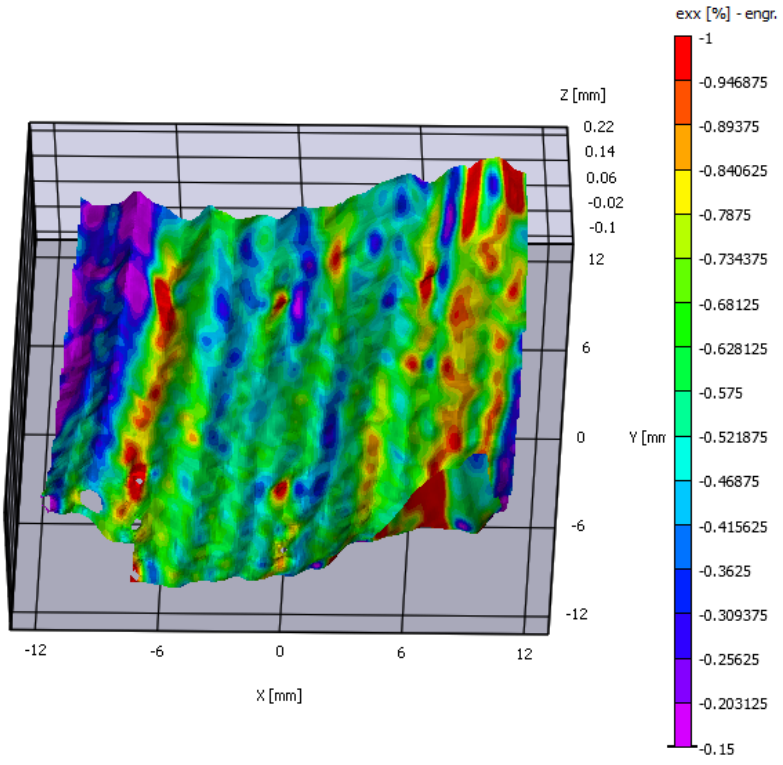

Figure 1: 3D DIC transvers strain map of the sample 15 minutes into the 60°C isothermal hold

3.1.2 Local variations

Upon preliminary examination, it is clear that the sample is not uniform at this stage in the heating cycle. Close examination of the strain map shows a repeating pattern in Δz, approximately every 4mm there is a peak in height. Variations in strain also appear showing higher than lower compressive strain in the transverse in-plane direction (ε_2), or the direction perpendicular to the fibres.

To explore the variations seen in Figure 1, points of interest are taken and used to analyze a local profile. Figure 2 shows the local variation of strain and change in the height of the sample during the isothermal hold portion of the heating cycle.

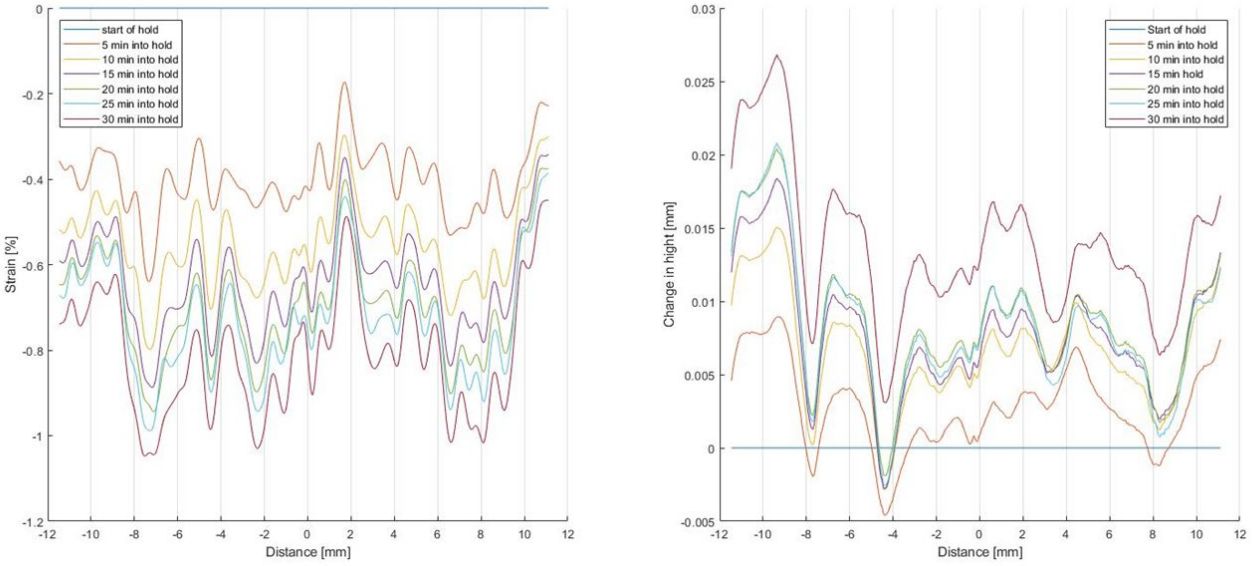

Figure 2: DIC local strain measurements taken along the width of the sample 8 mm from the bottom. (a) Development of local strain examined at 5 minute increments during the hold, using the start of the hold as reference.(b) Change in height examined at 5 minute increments during the hold, using the start of the hold as reference.

Focusing on the variation in magnitude of the change in height, there appears to be a peak every 4 mm. For AS4/8552, the tow size has been reported as 4mm, found using a resin burn off test (Stewart, 2018). This tow size value matches the apparent roughness of the material suggests the trend in Δz is induced by presence of the fiber tow. The strain pattern reported shows more frequent peaks than the Δz, approximately every 1mm. The variations in the strain plot show that in some areas the effects of shrinkage are more prominent than in other areas. Based on the knowledge of global behaviour, it is reasonable to think the local variations in strain could be indications of the morphology of the ply. Areas subject to high negative strain could be the result of resin being transported into void spaces. Further investigation into the morphology of the sample could inform the cause of this pattern.

3.1.3 Global variations

Figure 2 captures the local variation as well as the global behaviour. Globally, strain development over time shows shrinkage. Past studies have attributed global shrinkage to surface tension causing the resin to flow into void spaces in the dry prepreg core (Duffner et al., 2018; Zobeiry & Duffner, 2018).

Examining the global behaviour of Δz, over time the ply appears to increase in thickness as it shrinks in-plain.

3.1.4 SEM

An image of the prepreg morphology offers insight into the nonunivocity of the sample. SEM imaging provides a snapshot of the final morphology of a section of the sample after it has been heated. The resin and void distribution in the sample can be seen in Figure 3 which shows a portion of the cross-section.

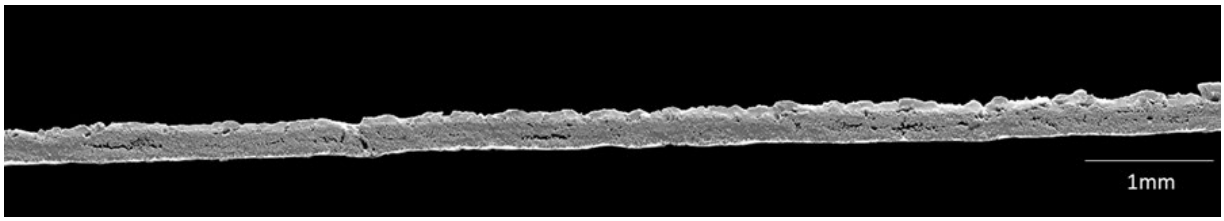

Figure 3:SEM image of a section of the AS4/8552 prepreg sample cross-section after heating cycle. Black spots are priority in the ply.

Using a Matlab image analysis routine, the void content can be found, and a plot of the size of void spaces over the sample is seen in Figure 4. In this sample, the average spacing between the large void spaces is 1 ±0.5mm, found by looking at the distance between the peaks on the curve.

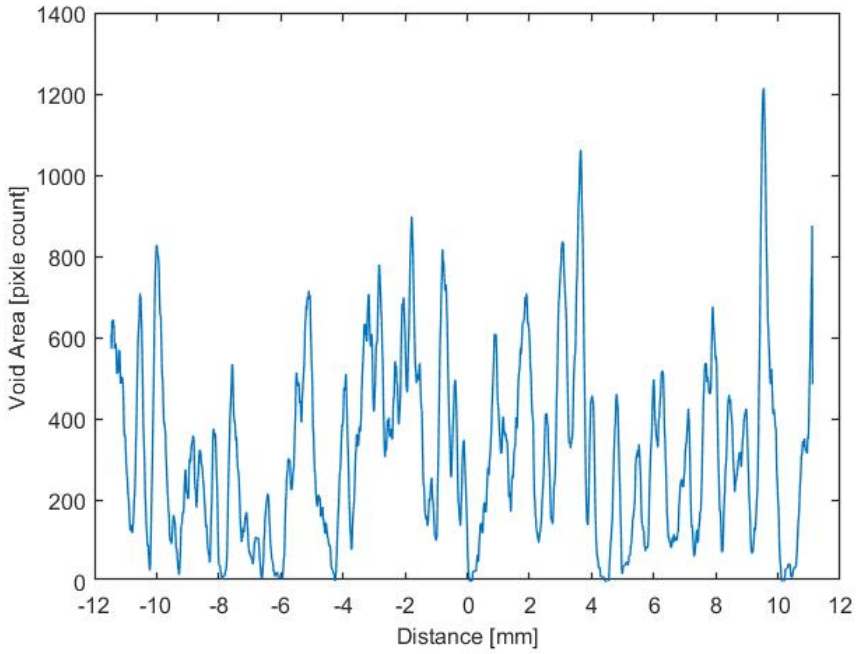

Figure 4 Void content over SEM cross-section. Peaks signify areas of high porosity, dips are areas with higher resin content.

It is important to note that the size of the void spaces and areas that are resin rich are not constant; a more robust data set is needed to identify the frequency between these critical features correctly. As this image represents the final morphology, it is also difficult to conclusively connect the porosity spacing to

the location of the tows however we do know the majority of the porosity can be found is in the tow region (Hernández et al., 2011).

3.1.5 Surface Characterization

The surface morphology can also provide information on non-uniformity of the strain and thickness of the sample during processing. Both Optical Microscopy and IR Imaging as seen in Figure 5 and Figure 6 respectively, show similar frequency surface patterns caused by resin rich areas. It is important to remember that the sample examined with these two techniques is cut from the same material, but is not the same sample that was examined in the previous methods.

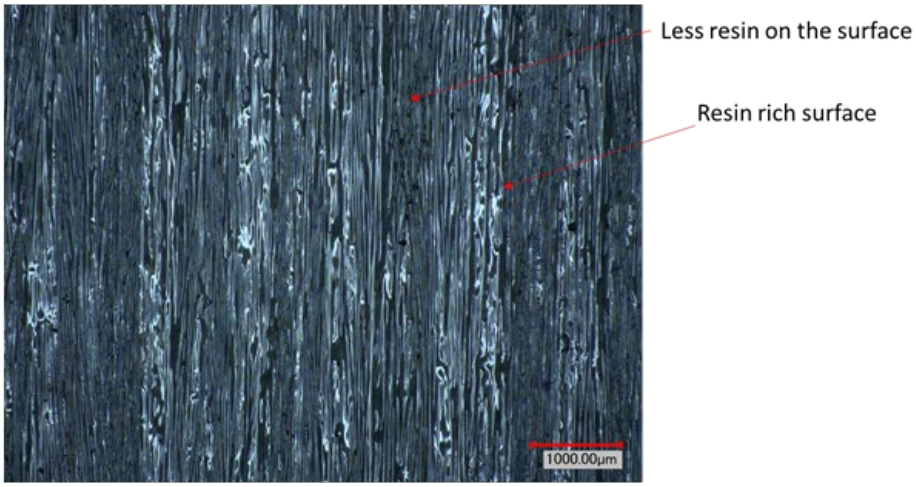

Figure 5: Optical Microscopy image of AS4/8552 prepreg surface.

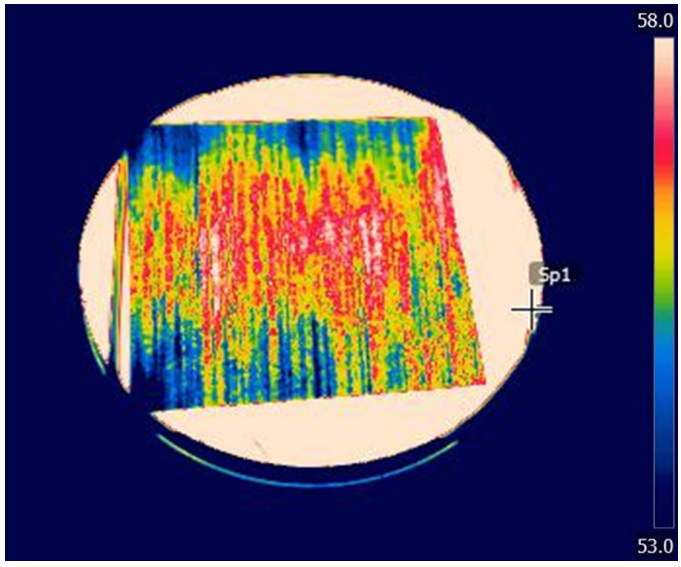

Figure 6: IR thermograph of AS4/8552 prepreg surface heated to approximately 60°C for 5 minutes.

The average spacing between resin rich areas seen on the surface of the prepreg using optical microscopy is found to be 1.1 ± 0.4mm. The resin will have a higher thermal conductivity to the fibres and so appear hotter. The IR image shows bands of hotter and colder regions on the sample as expected. The spacing between the hotter resin rich areas and the areas with fewer fibres averages to 1.2 ± 0.5mm.

Connecting the surface morphology back to the DIC strain experiments, it appears that the strain might be picking up the resin variation just as the IR and microscopy tests are. This seems reasonable as they are all techniques that look at the surface quality of the sample. More extensive tests are needed to correlate these effects properly. However, it seems promising that the surface morphology is matching the ply morphology. If accurate, this connection would be consistent with the past studies which observed trends in resin content and surface roughness (Helmus et al., 2017; Lukaszewicz & Potter, 2011).

4 CONCLUSION

The morphology of AS4/8552 prepreg was investigated to understand the effects the raw material has on the behaviour of the material. Experiments performed in this study used a variety of different methods; each give more information on the state of the material and suggested links between structures and observed behaviours. By examining the quality of the surface, a pattern in the resin distribution is seen, both IR and optical microscopy see a 1 mm spacing between resin rich areas on the surface of a ply of AS4/8552. The transverse in-plane strain also saw a repeating 1 mm spacing between peaks of larger shrinkage points. Although future work is needed to match the regions of higher strain to the resin rich areas, it is reasonable to assume that they are linked. Additionally, DIC results showed a link between the tow 4 mm size and the change in the height of the sample demonstrating that is a nondestructive method for finding this feature. Further work is still needed to connect the SEM microstructure to the strain and height patterns although it appears the location of resin rich areas in the core could be linked to the resin rich areas on the surface and the strain pattern.

Combining all the techniques in this study gives a better picture of the initial condition of the material. Although each method offers some bit of information, it is only when compared that patterns and trends become apparent. Traditionally the local changes are not focused on when thinking about creating process models for composite manufacturing, but as research starts to dig further into the initial condition of the material the importance in understanding all the interactions in this complex system before necessary and more attainable as each discovery offers new questions to be explored.

5 ACKNOWLEDGEMENTS

The authors would like to thank the Natural Sciences and Engineering Research Council of Canada (NSERC) along with the industrial members of the Composites Research Network (The Boeing Company, Convergent Manufacturing Technologies Inc., Toray Americas, Avcorp Industries) for their financial support. We would like to recognize our colleagues Dr. Goran Fernlund, Dr. Christophe Mobuchon, and Dr. Casey Keulen (Composites Research Network) for their continuous technical insights and recommendations.

REFERENCES

Convergent Manufacturting. (2017). RAVEN simulation software. Retrieved from http://www.convergent.ca/products/raven-simulation-software.

Correlated Solutions. (2010). Vic-3D 2010 Reference Manual, 107.

DUFFNER, C., ZOBEIRY, N., & POURSARTIP, A. (2018). Examination of Pre-gelation Behavior in AS4/8552 Prepreg Composites. "In Proceedings of the American Society for Composites—Thirty-third Technical Conference."

Helmus, R., Kratz, J., Potter, K., Hubert, P., & Hinterhölzl, R. (2017). An experimental technique to

characterize interply void formation in unidirectional prepregs. Journal of Composite Materials, 51(5), 579–591.

Hernández, S., Sket, F., Molina-Aldareguí a, J. M., González, C., & LLorca, J. (2011). Effect of curing cycle on void distribution and interlaminar shear strength in polymer-matrix composites. Composites Science and Technology, 71(10), 1331–1341.

HEXCEL. (2016). HexPly® 8552 Product Data Sheet. Hexcel, 1–6.

Lukaszewicz, D. H. J. A., & Potter, K. D. (2011). The internal structure and conformation of prepreg with respect to reliable automated processing. Composites Part A: Applied Science and Manufacturing, 42(3), 283–292.

Mohseni, S. M., Fernlund, G., & Lane, M. (2018). Cure cycle design to suppress moisture-driven bubble growth in polymer composites. Journal of Composite Materials, 52(13), 1821–1832.

Raffer, G. (2003). ROTARY RHEOMETER.

Stewart, A. L. (2018). Misalignment defects in unidirectioal composite materails. The University of British Columbia.

Stewart, A. L., & Poursartip, A. (2018). Characterization of fibre alignment in as-received aerospace grade unidirectional prepreg. Composites Part A: Applied Science and Manufacturing, 112, 239–249.

Van Ee, D., & Poursartip, A. (2009). NCAMP Hexply Material Properties Database for use with COMPRO CCA and Raven. National Center for Advanced Materials Performance, 141. Retrieved from http://www.niar.wichita.edu/coe/ncamp.asp%5Cnhttp://www.niar.wichita.edu/coe/ncamp_documents/Hexcel 8552/Hexcel8552MaterialCharacterizationBinderV0-9.pdf

Zobeiry, N., & Duffner, C. (2018). Measuring the negative pressure during processing of advanced composites. Composite Structures, 203.